Impact of anthropogenic emissions on biogenic secondary organic aerosol: Observation in the Pearl River Delta, South China

Yu-Qing Zhang[1, *], Duo-Hong Chen[2, *], Xiang Ding[1, †], Jun Li[1], Tao Zhang[2], Jun-Qi Wang[1], Qian Cheng[1], Hao Jiang[1], Wei Song[1], Yu-Bo Ou[2], Peng-Lin Ye[3], Gan Zhang[1], Xin-Ming Wang[1, 4]

1 State Key Laboratory of Organic Geochemistry and Guangdong Provincial Key Laboratory of Environmental Protection and Resources Utilization, Guangzhou Institute of Geochemistry, Chinese Academy of Sciences, Guangzhou, 510640, China

2 State Environmental Protection Key Laboratory of Regional Air Quality Monitoring, Environmental Monitoring Center of Guangdong Province, Guangzhou, 510308, China

3 Aerodyne Research Inc., Billerica, Massachusetts 01821, United States

4 Center for Excellence in Regional Atmospheric Environment, Institute of Urban Environment, Chinese Academy of Sciences, Xiamen, 361021, China

* These authors contributed equally to this work.

† *Correspondence to*: Xiang Ding (xiangd@gig.ac.cn)

Abstract. Secondary organic aerosol (SOA) formation from biogenic precursors is affected by anthropogenic emissions, which is not well understood in polluted areas. In the study, we accomplished a year-round campaign at nine sites in the polluted areas located in Pearl River Delta (PRD) region during 2015. We measured typical biogenic SOA (BSOA) tracers from isoprene, monoterpenes, and β-caryophyllene as well as major gaseous and particulate pollutants and investigated the impact of anthropogenic pollutants on BSOA formation. The concentrations of BSOA tracers were in the range of 45.4 to 109 ng m^{-3} with the majority composed of products from monoterpenes (SOA_M, 47.2 ± 9.29 ng m^{-3}), followed by isoprene (SOA_I, 23.1 ± 10.8 ng m^{-3}), and β-caryophyllene (SOA_C, 3.85 ± 1.75 ng m^{-3}). We found that atmospheric oxidants, O_x (O_3 plus NO_2), and sulfate correlated well with later-generation SOA_M tracers, but not so for first-generation SOA_M products. This suggested that high O_x and sulfate could promote the formation of later-generation SOA_M products, which probably led to relatively aged SOA_M we observed in the PRD. For the SOA_I tracers, not only 2-methylglyceric acid (NO/NO_2-channel product), but also the ratio of 2-methylglyceric acid to 2-methyltetrols (HO_2-channel products) exhibit NO_x dependence, indicating the significant impact of NO_x on SOA_I formation pathways. The SOA_C tracer elevated in winter at all sites and positively correlated with levoglucosan, O_x, and sulfate. Thus, the unexpected increase of SOA_C in wintertime might be highly associated with the enhancement of biomass burning, O_3 chemistry and sulfate component in the PRD. The BSOAs that were estimated by the SOA tracer approach showed the highest concentration in fall and the lowest concentration in spring with an annual average concentration of 1.68 ± 0.40 μg m^{-3}. SOA_M dominated the BSOA mass all year round. We also found that BSOA correlated well with sulfate and O_x. This implicated the significant effects of anthropogenic pollutants on BSOA formation and highlighted that we could reduce the BSOA through controlling on the anthropogenic emissions of sulfate and O_x precursors in polluted regions.

1 Introduction

Secondary organic aerosols (SOA) that are produced through homogenous and heterogeneous processes of volatile organic compounds (VOCs) have significant effects on global climate change and regional air quality (von Schneidemesser et al., 2015). Globally, the emissions of biogenic VOCs (BVOCs) are dominant over anthropogenic VOCs. Thus, biogenic SOA (BSOA) is predominant over anthropogenic SOA. In the past decade, laboratorial, field, and modeling studies have demonstrated that BSOA

formation is highly affected by anthropogenic emissions (Zhang et al., 2015; Hoyle et al., 2011; Carlton et al., 2010). Increasing NO_x shifts isoprene oxidation from the low-NO_x conditions to the high-NO_x conditions (Surratt et al., 2010) and enhances nighttime SOA formation via nitrate radical oxidation of monoterpenes (Xu et al., 2015). High SO_2 emission leads to abundant sulfate and acidic particles, which accelerates the BSOA production by the salting-in effect and acid-catalyzed reactions (Offenberg et al., 2009; Xu et al., 2016). In polluted regions, the increase of O_3 levels due to high emissions of NO_x and VOCs, likely results in significant SOA formation through the ozonolysis of BVOCs (Sipilä et al., 2014; Riva et al., 2017). In addition, large emission and formation of anthropogenic organic matter (OM) in urban areas enhance the incorporation of BVOCs' oxidation products into the condensed phase (Donahue et al., 2006). Recently, Carlton et al. (2018) found that the removal of anthropogenic emissions of NO_x, SO_2, and primary OA in the CMAQ simulations could reduce BSOA by 23, 14, and 8% in summertime, respectively.

The Pearl River Delta region (PRD) (Figure 1a) is the most developed region in China. Rapid economic growth during the past three decades has resulted in large amounts of anthropogenic emissions in the PRD (Lu et al., 2013). Our observation during fall-winter season in 2008 at a regional site of the PRD showed that daily $PM_{2.5}$ was as high as 150 μg m^{-3} (Ding et al., 2012). Fortunately, due to more and more strict and effective pollution controls in the PRD, $PM_{2.5}$ concentrations have significantly shrunk during the last decade and met the national ambient air quality standard (NAAQS) for annual-mean $PM_{2.5}$ (35 μg m^{-3}) since the year of 2015 (Figure 1b). However, O_3 and oxidant (O_x, $O_x = O_3 + NO_2$) are still in high levels and do not decrease apparently (Figure 1b). Hofzumahaus et al., (2009) observed extremely high OH concentrations in the PRD and proposed a recycling mechanism which increases the stability of OH in the air of polluted regions. All these indicate high atmospheric oxidative capacity in the PRD, since O_3, NO_x and OH are intimately linked in atmospheric chemistry. On the other hand, BVOCs emissions in the PRD are expected to be high all the year in such a subtropical area (Zheng et al., 2010). In the process of such a dramatic change in air pollution characteristics (e.g. $PM_{2.5}$ and O_3), BSOA origins and formation mechanisms in the PRD should be profoundly affected in the last decade. In this study, year-round $PM_{2.5}$ samples were collected at nine sites in the PRD during 2015. We investigated SOA tracers from typical BVOCs (isoprene, monoterpenes, and β-caryophyllene) across the PRD for the first time. We checked seasonal variations in concentrations and compositions of these BSOA tracers and evaluated the impact of anthropogenic pollutants on BSOAs formation in the PRD. We also accessed the

SOA origins and discussed the implication in further reducing BSOA through controlling on the anthropogenic emissions.

2 Experimental Section

2.1 Field Sampling

Concurrent sampling was performed at 9 out of 23 sites in the Guangdong-Hong Kong-Macao regional air quality monitoring network (http://www.gdep.gov.cn/hjjce/, Figure 1a), including three urban sites in Zhaoqing (ZQ), Guangzhou (GZ) and Dongguan (DG), two suburban sites in Nansha (NS) and Zhuhai (ZH), and four rural sites in Tianhu (TH), Boluo (BL), Heshan (HS) and Taishan (TS).

At each site, 24-hr sampling was conducted every six days from January to December in 2015 using a $PM_{2.5}$ sampler equipped with quartz filters (8 × 10 inches) at a flow rate of 1.1 m^3 min^{-1}. Additionally, field blanks were collected monthly at all sites. Blank filters were covered with aluminum foil and baked at 500 ºC for 12 hrs and stored in a container with silica gel. After sampling, the filter samples were stored at −20 ºC.

In this study, the filters collected in January, April, July and October 2015 were selected to represent winter, spring, summer, and fall samples, respectively. A total of 170 field samples (4-5 samples for each season at each site) were analyzed in the current study.

2.2 Chemical Analysis

For each filter, organic carbon (OC) and elemental carbon (EC) were measured by an OC-EC aerosol analyzer (Sunset Laboratory Inc.). Water-soluble ions were analyzed by ion chromatography (Metrohm). All these species are major components in $PM_{2.5}$ (see Figure 2). Meteorological parameters (temperature and relative humidity) and gaseous pollutants (SO_2, CO, NO_2, NO, and O_3) at each site were recorded hourly. We further calculated the daily averages to probe the potential influence of air pollutants on BSOA formation.

For BSOA tracer analysis, detailed information of the processes is described in the previous literatures (Shen et al., 2015; Ding et al., 2012). Isotope-labeled standard mixtures, including dodecanoic acid-d_{23}, hexadecanoic acid-d_{31}, docosanoic acid-d_{43} and levoglucosan-$^{13}C_6$ were added into each sample as internal standards. Then, samples were extracted by sonication with the mixed solvents of dichloride methane (DCM)/hexane (1:1, v/v) and DCM/methanol (1:1, v/v), sequentially. The extraction solutions

of each sample were combined, filtered, and concentrated to ~2 mL. Each concentrated sample was split into two parts for silylation and methylation, respectively.

We analyzed fourteen BSOA tracers in the derivatized samples using GC/MSD (Agilent 7890/5975C). The isoprene-derived SOA (SOA_I) tracers were composed of 2-methyltetrols (2-MTLs, 2-methylthreitol and 2-methylerythritol) (Claeys et al., 2004a), 2-methylglyceric acid (2-MGA) (Claeys et al., 2004b), 3-MeTHF-3,4-diols (*cis*-3-methyltetrahydrofuran-3,4-diol and *trans*-3-methyltetrahydrofuran-3,4-diol) (Lin et al., 2012) and C_5-alkene triols (*cis*-2-methyl-1,3,4-trihydroxy-1-butene, *trans*-2-methyl-1,3,4-trihydroxy-1-butene and 3-methyl-2,3,4-trihydroxy-1-butene) (Wang et al., 2005). The monoterpenes-derived SOA (SOA_M) tracers included 3-hydroxy-4,4-dimethylglutaric acid (HDMGA), 3-hydroxyglutaric acid (HGA) (Claeys et al., 2007), pinic acid (PA), *cis*-pinonic acid (PNA) (Christoffersen et al., 1998), and 3-methyl-1,2,3-butanetricarboxylic acid (MBTCA) (Szmigielski et al., 2007). The β-caryophyllene-derived SOA (SOA_C) tracer was β-caryophyllenic acid (CA) (Jaoui et al., 2007). Due to the lack of authentic standards, surrogate standards were used to quantify BSOA tracers except PNA. Specifically, erythritol, PNA and octadecanoic acid were used for the quantification of SOA_I tracers (Ding et al., 2008), other SOA_M tracers (Ding et al., 2014) and CA (Ding et al., 2011), respectively. The method detection limits (MDLs) for erythritol, PNA and octadecanoic acid were 0.01, 0.02, and 0.02 ng m^{-3}, respectively. Table S1 summarizes BSOA data at each site in the PRD.

2.3 Quality Assurance / Quality Control

These target BSOA tracers were not detected or lower than MDLs in the field blanks. The results of spiked samples (erythritol, PNA and octadecanoic acid spiked in pre-baked quartz filters) indicated that the recoveries were 65 ± 14 % for erythritol, 101 ± 3 % for PNA, and 83 ± 7 % for octadecanoic acid. The results of paired duplicate samples indicated that all the relative differences for target BSOA tracers were lower than 15%.

It should be noted that the application of surrogate quantification introduces additional errors to the results. Based on the empirical approach to calculate uncertainties from surrogate quantification (Stone et al., 2012), we estimated the errors in analyte measurement which were propagated from the uncertainties in field blanks, spike recoveries, repeatability and surrogate quantification. As Table S2 showed, the estimated uncertainties in the tracers' measurement ranged from 15% (PNA) to 157% (CA).

3 Results and Discussion

3.1 $PM_{2.5}$ and gaseous pollutants

Figure 2 presents spatial and seasonal variations of $PM_{2.5}$ and its major components. Although annual-mean $PM_{2.5}$ (34.8 ± 6.1 μg m^{-3}) in the PRD met the NAAQS value of 35 μg m^{-3}, $PM_{2.5}$ at the urban sites (ZQ, GZ and DG) all exceeded the NAAQS value. The rural TH site in the northern part of PRD witnessed the lowest concentration of $PM_{2.5}$ (25.0 μg m^{-3}) among the nine sites. $PM_{2.5}$ levels were highest in winter (on average 60.1 ± 21.6 μg m^{-3}) and lowest in summer (on average 22.8 ± 3.3 μg m^{-3}). Carbonaceous aerosols and water-soluble ions together explained 98 ± 11 % of $PM_{2.5}$ masses. OM (OC×1.6) was the most abundant component in $PM_{2.5}$, followed by sulfate, ammonium, nitrate and EC. Similar to $PM_{2.5}$, the five major components all increased in winter and fall (Figure S1), suggesting severe $PM_{2.5}$ pollution during fall-winter season in the PRD.

In the gas phase, SO_2, CO, NO_2 and NO_x presented similar seasonal trends as $PM_{2.5}$, i.e. higher levels occurred during fall and winter and lower concentrations during spring and summer (Figure 3 a-d). Annual-mean SO_2 and NO_2 in the PRD both met the NAAQS values of 60 μg m^{-3} and 40 μg m^{-3}, respectively (Figure 3a and 3c). As a typical secondary pollutant, O_3 was highest in summer (Figure 3e), probably because of the strong photo-chemistry. Due to the compromise of opposite seasonal trends of O_3 and NO_2, O_x showed less seasonal variation (Figure 3f) compared with other gaseous pollutants. And annual-mean O_x reached 96.1 ± 14.9 μg m^{-3}. These indicated significant O_3 pollution all the year in the PRD.

3.2 Spatial distribution and seasonal variation of SOA tracers

The total concentrations of BSOA tracers ranged from 45.4 to 109 ng m^{-3} among the nine sites. SOA_M tracers (47.2 ± 9.29 ng m^{-3}) represented predominance, followed by SOA_I tracers (23.1 ± 10.8 ng m^{-3}), and SOA_C tracer (3.85 ± 1.75 ng m^{-3}).

3.2.1 Monoterpenes-derived SOA tracers

Annual averages of total SOA_M tracers at the nine sites were in the range of 26.5 to 57.4 ng m^{-3} (Table S1). Figure 4 and Figure S2a show the spatial distribution of SOA_M tracers and monoterpene emissions in the PRD (Zheng et al., 2010). The highest concentration of SOA_M tracers was observed at the rural TH site where monoterpene emissions were high. Figure 4 also presents seasonal variations of SOA_M

tracers. At most sites, high levels occurred in summer and fall. Monoterpene emission rates are influenced by temperature and solar radiation (Guenther et al., 2012). Thus, high temperature and intensive solar radiation during summer and fall in the PRD (Zheng et al., 2010) could stimulate monoterpene emissions and then the SOA_M formation.

Among the five SOA_M tracers, HGA (20.1 ± 4.28 ng m^{-3}) showed the highest concentration, followed by HDMGA (14.7 ± 2.93 ng m^{-3}), MBTCA (7.63 ± 1.49 ng m^{-3}), PNA (3.75 ± 2.72 ng m^{-3}) and PA (1.01 ± 0.48 ng m^{-3}). SOA_M formation undergoes multi-generation reactions. The first-generation SOA_M (SOA_{M_F}) products, PNA and PA, can be further oxidized and form the later-generation (SOA_{M_L}) products, e.g. MBTCA (Müller et al., 2012). Thus, the (PNA+PA) / MBTCA ratio has been used to probe SOA_M aging (Haque et al., 2016; Ding et al., 2014). The (PNA+PA) / MBTCA ratios in chamber-generated α-pinene SOA samples were reported in the range of 1.51 to 5.91 depending on different oxidation conditions (Offenberg et al., 2007; Eddingsaas et al., 2012). In this study, the median values of (PNA+PA) / MBTCA varied from 0.27 at ZH to 1.67 at TH. The ratios observed in this study were consistent with our previous observations at the regional site, Wanqingsha (WQS) in the PRD (Ding et al., 2012), but lower than those in the fresh α-pinene SOA samples from chamber experiments (Figure S3), indicating relatively aged SOA_M in the air of PRD.

Moreover, the levels of SOA_{M_L} tracers (HGA + HDMGA + MBTCA) were much higher than those of SOA_{M_F} tracers (PNA + PA), with mean mass fractions of SOA_{M_L} tracers reaching 86% (Figure 4). Mass fractions of SOA_{M_F} tracers decreased in the summer samples (Figure 4), probably resulting from strong photo-chemistry and more intensive further oxidation during summer. High abundances of SOA_{M_L} tracers in the PRD were different from our year-round observations at 12 sites across China (Ding et al., 2016b). In that study, the (PNA+PA) / MBTCA ratio suggested generally fresh SOA_M (Figure S3) and SOA_{M_F} tracers were the majority. Thus, we see more aged SOA_M in the PRD.

As Figure 5 a-b and Figure S4,S5 showed, the SOA_{M_F} tracers did not show good correlations with O_x at most sites, while the SOA_{M_L} tracers exhibited significant O_x dependence. When O_x is high, strong photo-oxidation of PNA and PA could reduce their concentrations and promote the formation of SOA_{M_L} tracers (Müller et al., 2012). Thus, the levels of SOA_{M_L} tracers would increase with increasing O_x but not so for SOA_{M_F} tracers. On the other hand, sulfate is a key species in particles that determines aerosol liquid water amount, aerosol acidity, and particle surface area (Xu et al., 2015, 2016). Thus, the increase of sulfate could promote aqueous and heterogeneous reactions. In this study, the SOA_{M_F} tracers poorly

correlated with sulfate (Figure 5c), while the SOA_{M_L} tracers positively correlated with sulfate at all the 9 sites (Figure 5d). At each site the SOA_{M_L} tracers exhibited more sulfate dependence than the SOA_{M_F} tracers (Figure S5). This suggested that sulfate also played a critical role in forming SOA_{M_L} tracers through the particle-phase reactions. Besides the gas-phase OH oxidation (Müller et al., 2012), the heterogeneous OH oxidation of pinonic acid could also produce SOA_{M_L} tracers (Lai et al. 2015). Aljawhary et al., (2016) reported the kinetics and mechanism of pinonic acid oxidation in acidic solutions and found that the molar yields of MBTCA through the aqueous-phase reactions were similar to those in the gas-phase oxidation. Here, we conclude that high concentrations of O_x and sulfate could stimulate SOA_{M_L} tracers' production and thereby lead to aged SOA_M in the PRD.

3.2.2 Isoprene-derived SOA tracers

Annual averages of total SOA_I tracers at the nine sites were in the range of 10.8 to 49.3 ng m^{-3} (Table S1). Figure 6 and Figure S2b show the spatial distribution of SOA_I tracers and isoprene emissions in the PRD (Zheng et al., 2010), respectively. The highest concentration occurred at ZQ where the emissions were high. Figure 6 also presents seasonal variations of SOA_I tracers at the nine sites. High levels occurred in summer and fall. Similar to monoterpenes, the emission rate of isoprene is influenced by temperature and solar radiation (Guenther et al., 2012), which are expected to be higher in summer and fall in the PRD (Zheng et al., 2010). Among these SOA_I tracers, 2-MTLs (14.2 ± 5.61 ng m^{-3}) were the most abundant products, followed by C_5-alkene triols (6.81 ± 5.05 ng m^{-3}), 2-MGA (1.99 ± 0.72 ng m^{-3}) and 3-MeTHF-3,4-diols (0.19 ± 0.08 ng m^{-3}).

SOA_I formation is highly affected by NO_x (Surratt et al., 2010). Under the low-NO_x or NO_x free conditions, isoprene is oxidized by the OH and HO_2 radicals through the HO_2-channel which generates a hydroxy hydroperoxide (ISOPOOH) and then forms epoxydiols (IEPOX) (Paulot et al., 2009). Reactive uptake of IEPOX on acidic particles eventually produces 2-MTLs, C_5-alkene triols, 3-MeTHF-3,4-diols, 2-MTLs-organosulfates and oligomers (Lin et al., 2012). Under the high-NO_x conditions, isoprene undergoes oxidation by NO_x through the NO/NO_2-channel and generates methacrolein (MACR) and then forms peroxymethylacrylic nitric anhydride (MPAN). Further oxidation of MPAN by the OH radical produces hydroxymethel-methyl-α-lactone (HMML) and/or methacrylic acid epoxide (MAE). HMML and MAE are the direct precursors to 2-MGA, 2-MGA-organosulfate and its corresponding oligomers (Nguyen et al., 2015). As Figure 6 showed, the concentrations of HO_2-channel tracers (2-MTLs + C_5-

alkene triols + 3-MeTHF-3,4-diols) were much higher than those of the NO/NO_2-channel product (2-MGA) at all the nine sites. The dominance of HO_2-channel products was also observed at another regional site in the PRD (WQS) (He et al., 2018).

Figure 6 also shows seasonal trends of the 2-MGA to 2-MTLs ratio (2-MGA/2-MTLs) which is often applied to probe the influence of NO_x on the formation of SOA_I (Ding et al., 2013; Ding et al., 2016a; Pye et al., 2013). The ratios were highest in wintertime and lowest in summertime, which were consistent with the seasonal trend of NO_x during our campaign (Figure 3d). As Table 1 showed, 2-MGA positively correlated with NO_2, probably due to the enhanced formation of MPAN from peroxymethacryoyl (PMA) radical reacted with NO_2 (Worton et al., 2013; Chan et al., 2010). Previous laboratory studies showed that increasing NO_2/NO ratio could promote the formation of 2-MGA and its corresponding oligoesters (Chan et al., 2010; Surratt et al., 2010). However, we did not see a significant correlation between 2-MGA and NO_2/NO ratio in the PRD. Instead, the 2-MGA/2-MTLs ratio correlated well with NO, NO_2 and NO_2/NO ratio (Table 1). Increasing NO limits the formation of ISOPOOH but prefers the production of MACR, and increasing NO_2 enhances MPAN formation. Thus, it is expected that the 2-MGA/2-MTLs ratio shows stronger NO_x dependence than 2-MGA. These findings demonstrate the significant impact of NO_x on SOA_I formation pathways in the atmosphere. We also checked the correlations of SOA_I tracers with O_x and sulfate (Figure S6). The NO/NO_2-channel product exhibited more O_x and sulfate dependance than HO_2-channel products.

Recent studies indicated that isoprene ozonolysis might play a role in SOA_I formation in the ambient air. Riva et al. (2016) found that isoprene ozonolysis with acidic particles could produce substantial 2-MTLs but not so for C_5-alkene triols and 3-MeTHF-3,4-diols. Li et al. (2018) observed a positive correlation between 2-MTLs and O_3 in the North China Plain. In the PRD, we also saw weak but significant correlations of 2-MTLs with O_3 (Table S3). However, 3-MeTHF-3,4-diols and C_5-alkene triols were detected in all samples and 2-MTLs, C_5-alkene triols and 3-MeTHF-3,4-diols correlated well with each other (Table S4), which was apparently different from those reported by Riva et al. (2016). Moreover, the ratios of 2-MTLs isomers in the PRD samples (2.00−2.85) were much lower than those (10−22, Figure S7) reported in the SOA from isoprene ozonolysis (Riva et al., 2016). Furthermore, isoprene oxidation by the OH radical is much faster than that by ozone under the polluted PRD conditions (Table S5). And IEPOX yields through the ISOPOOH oxidation by the OH radical are more than 75% in the atmosphere (St. Clair et al., 2016). Thus, isoprene ozonolysis might be not the major formation

pathway of SOA_I, even though annual-mean O_3 level reaching 67.7 μg m^{-3} in the PRD (Table S1).

Previous studies found that thermal decomposition of low volatility organics in IEPOX-derived SOA could produce SOA_I tracers, e.g. 2-MTLs, C_5-alkene triols and 3-MeTHF-3,4-diols (Lopez-Hilfiker et al., 2016, Watanabe et al., 2018). This means that these tracers detected by GC-MSD might be generated from thermal decomposition of IEPOX-derived SOA. As estimated by Cui et al (2018), 14.7-42.8% of C_5-alkene triols, 11.1% of 2-MTLs and approximately all 3-MeTHF-3,4-diols.measured by GC/ MSD could be attributed to the thermal degradation of 2-MTLs-derived organosulfates (MTL-OSs). We also measured MTL-OSs in two samples at HS and TS sites, respectively (Table S6) using the widely used LC-MS approach (He et al., 2014, 2018). Assuming that all MTL-OSs decomposed to these tracers, the thermal decomposition of MTL-OSs would account for 15.1-31.6% of C_5-alkene triols, 6.0-10.0% of 2-MTLs and all 3-MeTHF-3,4-diols measured by GC/ MSD. Thus, C_5-alkene triols and 2-MTLs are major from isoprene oxidation rather than thermal decomposition of MTL-OSs, while 3-MeTHF-3,4-diols are only in trace amount in the air and might be produced largely from thermal degradation.

Moreover, we see significant variations in SOA_I tracer compositions in the PRD. For instant, C_5-alkene triols have three isomers. If these tracers were mainly generated from a thermal process, their compositions should be similar in different samples. In fact, the relative abundances of three C_5-alkene triol isomers significantly changed from site to site (Figure 7) and season to season (Figure S8), and their compositions in the PRD were different from those measured in the chamber samples (Lin et al., 2012). In addition, the slopes of linear correlations among these IEPOX-derived SOA tracers also varied from site to site (Figure S9). Coupled with the seasonal trend of 2-MGA/2-MTLs ratios, the apparent variations in SOA_I tracer compositions demonstrate that these SOA_I tracers are mainly formed through different pathways in the ambient atmosphere, although part of them might arise from the thermal decomposition of different dimers/OSs and the parent dimers/OSs varies with sites and seasons.

3.2.3 Sesquiterpene-derived SOA tracer

Annual averages of CA at the nine sites ranged from 1.82 to 7.07 ng m^{-3}. The levels of CA at the inland sites (e.g. GZ, ZQ, and TH) were higher than those at the coastal sites (ZH and NS, Figure 8). Since sesquiterpenes are typical BVOCs, it is unexpected that the concentrations of CA were highest during winter in the PRD (Figure 8). Interestingly, seasonal trend of CA was consistent with that of the biomass burning (BB) tracer, levoglucosan (Figure 8). And CA correlated well with levoglucosan at eight sites in

the PRD (Figure 9a). Sesquiterpenes are stored in plant tissues partly to protect the plants from insects and pathogens (Keeling and Bohlmann, 2006). BB can not only stimulate sesquiterpene emissions (Ciccioli et al., 2014) but also substantially alter the SOA formation and yields (Mentel et al., 2013). Emissions inventories in the PRD showed that the BB emissions were enhanced during winter (He et al., 2011). These suggested that the unexpected increase of SOA_C in wintertime could be highly associated with BB emissions in the PRD.

Besides the impact of BB, we also found positive correlations of CA with O_x (Figure 9b) and sulfate (Figure 9c). The oxidation of β-caryophyllene by the OH radical and O_3 is very rapid. Under typical oxidation conditions in the air of PRD, the lifetimes of β-caryophyllene are only several minutes (Table S5). Once emitted from vegetation or biomass burning, β-caryophyllene will reacted rapidly and form CA immediately. This partly explains the positive correlations between CA and levoglucosan in the PRD. The unexpected high levels of CA in the winter indicated that biomass burning could be an important source of SOA_C in the PRD, especially in wintertime. In addition, the increase of sulfate could raise aerosol acidity and thereby promote aqueous and heterogeneous reactions to form SOA_C. In the PRD, both O_x (Figure 3f) and sulfate (Figure S1) increased during winter, which could promote SOA_C formation. Here, we conclude that the enhancement of BB emissions as well as the increase of O_x and sulfate in wintertime together led to high SOA_C production during winter in the PRD.

3.3 Source apportionment and atmospheric implications

We further attributed BSOA by the SOA-tracer approach which was first developed by Kleindienst et al. (2007). This method has applied to SOA apportionment at multiple sites across the United States (Lewandowski et al., 2013) and China (Ding et al., 2016b), and over global oceans from Arctic to Antarctic (Hu et al., 2013). Details of the SOA-tracer method and its application in this study as well as the uncertainty of estimating procedure are described in Text S1. Table S1 lists the results of estimated SOA from different BVOCs.

Figure 10a exhibits the spatial distribution of BSOA (SOA_M + SOA_I + SOA_C). Annual average at the nine sites ranged from 0.97 μg m^{-3} (NS) to 2.19 μg m^{-3} (ZQ), accounting for 9-15% of OM. SOA_M was the largest BSOA contributor with an average contribution of 64 ± 7 %, followed by SOA_C (21 ± 6 %), and SOA_I (14 ± 4 %). Figure 10b presents seasonal variation of BSOA. The levels were highest in fall (2.35 ± 0.95 μg m^{-3}) and lowest in spring (1.06 ± 0.42 μg m^{-3}). SOA_M contributions ranged from 57%

in winter to 68% in spring. The shares of SOA_I were only 5% in winter and reached up to 22% in summer. The contributions of SOA_C increased to 40% in wintertime.

It is interesting to note that SOA_M, SOA_I and SOA_C all positively correlated with sulfate and O_x in the PRD (Table 2). Since anthropogenic emissions can enhance BSOA formation (Hoyle et al., 2011), the reduction of anthropogenic emissions indeed lowers BSOA production (Carlton et al., 2018). As the oxidation product of SO_2, sulfate is a key species in particles that determines aerosol acidity and surface areas (Xu et al., 2015, 2016) which could promotes BSOA formation through the acid-catalyzed heterogeneous reactions. Recent study found that SO_2 could directly reaction with organic peroxides of monoterpene ozonolysis and form substantial organosulfates (Ye et al., 2018). Thus, the decrease of SO_2 emission indeed reduces SO_2 and sulfate in the ambient air, which hereby leads to less acidic particles and reduces the BSOA production. For O_x, the increase of O_3 likely results in significant SOA formation through the BVOCs ozonolysis (Sipilä et al., 2014; Riva et al., 2017). Hence, the decrease of O_x resulting from the control of VOCs and NO_x emissions could reduce BSOA formation through O_3 chemistry. Based on the observed sulfate and O_x dependence of BSOA in this study, the reduction of 1 μg m^{-3} in sulfate and O_x in the air of PRD could lower BSOA levels by 0.17 and 0.02 μg m^{-3}, respectively. If both concentrations decline by 50%, the reduction of O_x is more efficient than sulfate in reducing BSOA in the PRD (Table 2).

We further compared the results in 2015 with those during fall-winter season in 2008 at WQS (Ding et al., 2012). We found that all BSOA species positively correlated with sulfate but exhibited no O_x dependence (Table S7). Thus, in 2008 BSOA formation was largely influenced by sulfate, probably due to high sulfate levels then (as high as 46.8 μg m^{-3}). Owing to strict control of SO_2 emissions (Wang et al., 2013), ambient SO_2 significantly shrank over the PRD (Figure 1b). Our long-term observation during fall-winter season at WQS also witnessed a decreasing trend of sulfate from 2007 to 2016 (Figure S10). However, O_x levels did not decrease during the past decade (Figure 1b) and O_x concentrations were much higher than sulfate in 2015 in the PRD (96.1 ± 14.9 μg m^{-3} vs. 8.44 ± 1.09 μg m^{-3} on average). All these underline the importance of O_x in BSOA formation currently in the PRD. At present, short-term despiking and long-term attainment of O_3 concentrations are challenges for air pollution control in the PRD (Ou et al., 2016). Thus, lowering O_x is critical to improve air quality in the PRD. Our results highlight the importance of future reduction in anthropogenic pollutant emissions (e.g. SO_2 and O_x precursors) for considerably reducing the BSOA burden in polluted regions.

Code/Data availability

The experimental data in this study are available upon request to the corresponding author by email.

Author Contribution

Xiang Ding, Duo-Hong Chen and Jun Li conceived the project and designed the study. Yu-Qing Zhang and Duo-Hong Chen performed the data analysis and wrote the manuscript. Duo-Hong Chen, Tao Zhang and Yu-Bo Ou arranged the sample collection and assisted with the data analysis. Jun-Qi Wang, Qian Cheng and Hao Jiang analyzed the samples. Xiang Ding, Peng-Lin Ye, Wei Song, Gan Zhang and Xin-Ming Wang performed data interpretation and edited the manuscript. All authors contributed to the final manuscript development.

Competing interests

The authors declare that they have no conflict of interest.

Acknowledgments

This study was supported by National Key Research and Development Program (2018YFC0213902), National Natural Science Foundation of China (41722305/41603070/41473099), and Local Innovative and Research Teams Project of Guangdong Pearl River Talents Program (NO. 2017BT01Z134). We would like to thank Prof. Sasho Gligorovski for his helpful suggestion on the discussion of atmospheric oxidation process. The data of gaseous pollutants, major components in $PM_{2.5}$ and BSOA tracers can be found in supporting information.

References

Aljawhary, D., Zhao, R., Lee, A. K. Y., Wang, C., and Abbatt, J. P. D.: Kinetics, mechanism, and secondary organic aerosol yield of aqueous phase photo-oxidation of α-pinene oxidation products, J. Phys. Chem. A., 120, 1395-1407, 10.1021/acs.jpca.5b06237, 2016.

Carlton, A. G., Pinder, R. W., Bhave, P. V., and Pouliot, G. A.: To what extent can biogenic SOA be controlled?, Environ. Sci. Technol., 44, 3376-3380, 10.1021/es903506b, 2010.

Carlton, A. G., Pye, H. O. T., Baker, K. R., and Hennigan, C. J.: Additional benefits of federal air-quality

rules: Model estimates of controllable biogenic secondary organic aerosol, Environ. Sci. Technol., 52, 9254-9265, 10.1021/acs.est.8b01869, 2018.

Chan, A. W. H., Chan, M. N., Surratt, J. D., Chhabra, P. S., Loza, C. L., Crounse, J. D., Yee, L. D., Flagan, R. C., Wennberg, P. O., and Seinfeld, J. H.: Role of aldehyde chemistry and NO_x concentrations in secondary organic aerosol formation, Atmos. Chem. Phys., 10, 7169-7188, 10.5194/acp-10-7169-2010, 2010.

Christoffersen, T. S., Hjorth, J., Horie, O., Jensen, N. R., Kotzias, D., Molander, L. L., Neeb, P., Ruppert, L., Winterhalter, R., Virkkula, A., Wirtz, K., and Larsen, B. R.: Cis-pinic acid, a possible precursor for organic aerosol formation from ozonolysis of α-pinene, Atmos. Environ., 32, 1657-1661, https://doi.org/10.1016/S1352-2310(97)00448-2, 1998.

Ciccioli, P., Centritto, M., and Loreto, F.: Biogenic volatile organic compound emissions from vegetation fires, Plant Cell Environ., 37, 1810-1825, 10.1111/pce.12336, 2014.

Claeys, M., Graham, B., Vas, G., Wang, W., Vermeylen, R., Pashynska, V., Cafmeyer, J., Guyon, P., Andreae, M. O., Artaxo, P., and Maenhaut, W.: Formation of secondary organic aerosols through photooxidation of isoprene, Science, 303, 1173-1176, 10.1126/science.1092805, 2004a.

Claeys, M., Wang, W., Ion, A. C., Kourtchev, I., Gelencsér, A., and Maenhaut, W.: Formation of secondary organic aerosols from isoprene and its gas-phase oxidation products through reaction with hydrogen peroxide, Atmos. Environ., 38, 4093-4098, https://doi.org/10.1016/j.atmosenv.2004.06.001, 2004b.

Claeys, M., Szmigielski, R., Kourtchev, I., Van der Veken, P., Vermeylen, R., Maenhaut, W., Jaoui, M., Kleindienst, T. E., Lewandowski, M., Offenberg, J. H., and Edney, E. O.: Hydroxydicarboxylic acids: Markers for secondary organic aerosol from the photooxidation of α-pinene, Environ. Sci. Technol., 41, 1628-1634, 10.1021/es0620181, 2007.

Cui, T., Zeng, Z., dos Santos, E. O., Zhang, Z., Chen, Y., Zhang, Y., Rose, C. A., Budisulistiorini, S. H., Collins, L. B., Bodnar, W. M., de Souza, R. A. F., Martin, S. T., Machado, C. M. D., Turpin, B. J., Gold, A., Ault, A. P., and Surratt, J. D.: Development of a hydrophilic interaction liquid chromatography (HILIC) method for the chemical characterization of water-soluble isoprene epoxydiol (IEPOX)-derived secondary organic aerosol, Environ. Sci.: Processes Impacts, 20, 1524-1536, 10.1039/C8EM00308D, 2018.

Ding, X., Zheng, M., Yu, L., Zhang, X., Weber, R. J., Yan, B., Russell, A. G., Edgerton, E. S., and Wang,

X.: Spatial and seasonal trends in biogenic secondary organic aerosol tracers and water-soluble organic carbon in the southeastern United States, Environ. Sci. Technol., 42, 5171-5176, 10.1021/es7032636, 2008.

Ding, X., Wang, X., and Zheng, M.: The influence of temperature and aerosol acidity on biogenic secondary organic aerosol tracers: Observations at a rural site in the central Pearl River Delta region, South China, Atmos. Environ., 45, 1303-1311, 10.1016/j.atmosenv.2010.11.057, 2011.

Ding, X., Wang, X., Gao, B., Fu, X., He, Q., Zhao, X., Yu, J., and Zheng, M.: Tracer based estimation of secondary organic carbon in the Pearl River Delta, South China, J. Geophys. Res-Atmos., 117, D05313, 10.1029/2011JD016596, 2012.

Ding, X., Wang, X., Xie, Z., Zhang, Z., and Sun, L.: Impacts of Siberian biomass burning on organic aerosols over the North Pacific Ocean and the Arctic: Primary and secondary organic tracers, Environ. Sci. Technol., 47, 3149-3157, 10.1021/es3037093, 2013.

Ding, X., He, Q. F., Shen, R. Q., Yu, Q. Q., and Wang, X. M.: Spatial distributions of secondary organic aerosols from isoprene, monoterpenes, β-caryophyllene, and aromatics over China during summer, J. Geophys. Res-Atmos., 119, 11877-11891, 10.1002/2014JD021748, 2014.

Ding, X., He, Q. F., Shen, R. Q., Yu, Q. Q., Zhang, Y. Q., Xin, J. Y., Wen, T. X., and Wang, X. M.: Spatial and seasonal variations of isoprene secondary organic aerosol in China: Significant impact of biomass burning during winter, Sci. Rep., 6, 20411, 10.1038/srep20411, 2016a.

Ding, X., Zhang, Y. Q., He, Q. F., Yu, Q. Q., Shen, R. Q., Zhang, Y., Zhang, Z., Lyu, S. J., Hu, Q. H., Wang, Y. S., Li, L. F., Song, W., and Wang, X. M.: Spatial and seasonal variations of secondary organic aerosol from terpenoids over China, J. Geophys. Res-Atmos., 121, 14661–14678, 10.1002/2016JD025467, 2016b.

Donahue, N. M., Robinson, A. L., Stanier, C. O., and Pandis, S. N.: Coupled partitioning, dilution, and chemical aging of semivolatile organics, Environ. Sci. Technol., 40, 2635-2643, 10.1021/es052297c, 2006.

Eddingsaas, N. C., Loza, C. L., Yee, L. D., Chan, M., Schilling, K. A., Chhabra, P. S., Seinfeld, J. H., and Wennberg, P. O.: α-pinene photooxidation under controlled chemical conditions – Part 2: SOA yield and composition in low- and high-NO_x environments, Atmos. Chem. Phys., 12, 7413-7427, 10.5194/acp-12-7413-2012, 2012.

Guenther, A. B., Jiang, X., Heald, C. L., Sakulyanontvittaya, T., Duhl, T., Emmons, L. K., and Wang, X.:

The model of emissions of gases and aerosols from nature version 2.1 (MEGAN2.1): an extended and updated framework for modeling biogenic emissions, Geosci. Model. Dev., 5, 1471-1492, 10.5194/gmd-5-1471-2012, 2012.

Haque, M. M., Kawamura, K., and Kim, Y.: Seasonal variations of biogenic secondary organic aerosol tracers in ambient aerosols from Alaska, Atmos. Environ., 130, 95-104, 10.1016/j.atmosenv.2015.09.075, 2016.

He, M., Zheng, J., Yin, S., and Zhang, Y.: Trends, temporal and spatial characteristics, and uncertainties in biomass burning emissions in the Pearl River Delta, China, Atmos. Environ., 45, 4051-4059, 10.1016/j.atmosenv.2011.04.016, 2011.

He, Q. F., Ding, X., Wang, X. M., Yu, J. Z., Fu, X. X., Liu, T. Y., Zhang, Z., Xue, J., Chen, D. H., Zhong, L. J., and Donahue, N. M.: Organosulfates from pinene and isoprene over the Pearl River Delta, South China: Seasonal variation and implication in formation mechanisms, Environ. Sci. Technol., 48, 9236-9245, 10.1021/es501299v, 2014.

He, Q. F., Ding, X., Fu, X. X., Zhang, Y. Q., Wang, J. Q., Liu, Y. X., Tang, M. J., Wang, X. M., and Rudich, Y.: Secondary organic aerosol formation from isoprene epoxides in the Pearl River Delta, South China: IEPOX- and HMML− derived tracers, J. Geophys. Res-Atmos., 123, 6999-7012, 10.1029/2017JD028242, 2018.

Hofzumahaus, A., Rohrer, F., Lu, K., Bohn, B., Brauers, T., Chang, C.-C., Fuchs, H., Holland, F., Kita, K., Kondo, Y., Li, X., Lou, S., Shao, M., Zeng, L., Wahner, A., and Zhang, Y.: Amplified trace gas removal in the troposphere, Science, 324, 1702-1704, 10.1126/science.1164566, 2009.

Hoyle, C. R., Boy, M., Donahue, N. M., Fry, J. L., Glasius, M., Guenther, A., Hallar, A. G., Huff Hartz, K., Petters, M. D., Petäjä, T., Rosenoern, T., and Sullivan, A. P.: A review of the anthropogenic influence on biogenic secondary organic aerosol, Atmos. Chem. Phys., 11, 321-343, 10.5194/acp-11-321-2011, 2011.

Hu, Q. H., Xie, Z. Q., Wang, X. M., Kang, H., He, Q. F., and Zhang, P.: Secondary organic aerosols over oceans via oxidation of isoprene and monoterpenes from Arctic to Antarctic, Sci. Rep., 3, 2280, 10.1038/srep02280, 2013.

Jaoui, M., Lewandowski, M., Kleindienst, T. E., Offenberg, J. H., and Edney, E. O.: β-caryophyllinic acid: An atmospheric tracer for β-caryophyllene secondary organic aerosol, Geophys. Res. Let., 34, 10.1029/2006gl028827, 2007.

Keeling, C. I., and Bohlmann, J.: Genes, enzymes and chemicals of terpenoid diversity in the constitutive and induced defence of conifers against insects and pathogens, New Phytol., 170, 657-675, 10.1111/j.1469-8137.2006.01716.x, 2006.

Kleindienst, T. E., Jaoui, M., Lewandowski, M., Offenberg, J. H., Lewis, C. W., Bhave, P. V., and Edney, E. O.: Estimates of the contributions of biogenic and anthropogenic hydrocarbons to secondary organic aerosol at a southeastern US location, Atmos. Environ., 41, 8288-8300, 10.1016/j.atmosenv.2007.06.045, 2007.

Lai, C., Liu, Y., Ma, J., Ma, Q., Chu, B., and He, H.: Heterogeneous kinetics of cis-pinonic acid with hydroxyl radical under different environmental conditions, J. Phys. Chem. A., 119, 6583-6593, 10.1021/acs.jpca.5b01321, 2015.

Lewandowski, M., Piletic, I. R., Kleindienst, T. E., Offenberg, J. H., Beaver, M. R., Jaoui, M., Docherty, K. S., and Edney, E. O.: Secondary organic aerosol characterisation at field sites across the United States during the spring–summer period, Int. J. Environ. An. Ch., 93, 1084-1103, 10.1080/03067319.2013.803545, 2013.

Li, J., Wang, G., Wu, C., Cao, C., Ren, Y., Wang, J., Li, J., Cao, J., Zeng, L., and Zhu, T.: Characterization of isoprene-derived secondary organic aerosols at a rural site in North China Plain with implications for anthropogenic pollution effects, Sci. Rep., 8, 535, 10.1038/s41598-017-18983-7, 2018.

Lin, Y.-H., Zhang, Z., Docherty, K. S., Zhang, H., Budisulistiorini, S. H., Rubitschun, C. L., Shaw, S., Knipping, E., Edgerton, E. S., Kleindienst, T. E., Gold, A., and Surratt, J. D.: Isoprene epoxydiols as precursors to secondary organic aerosol formation: Acid-catalyzed reactive uptake studies with authentic standards, Environ. Sci. Technol., 46, 189-195, 10.1021/es202554c, 2012.

Lopez-Hilfiker, F. D., Mohr, C., D'Ambro, E. L., Lutz, A., Riedel, T. P., Gaston, C. J., Iyer, S., Zhang, Z., Gold, A., Surratt, J. D., Lee, B. H., Kurten, T., Hu, W. W., Jimenez, J., Hallquist, M., and Thornton, J. A.: Molecular composition and volatility of organic aerosol in the southeastern U.S.: Implications for IEPOX derived SOA, Environ. Sci. Technol., 50, 2200-2209, 10.1021/acs.est.5b04769, 2016.

Lu, Q., Zheng, J., Ye, S., Shen, X., Yuan, Z., and Yin, S.: Emission trends and source characteristics of SO_2, NO_x, PM_{10} and VOCs in the Pearl River Delta region from 2000 to 2009, Atmos. Environ., 76, 11-20, 10.1016/j.atmosenv.2012.10.062, 2013.

Müller, L., Reinnig, M. C., Naumann, K. H., Saathoff, H., Mentel, T. F., Donahue, N. M., and Hoffmann, T.: Formation of 3-methyl-1,2,3-butanetricarboxylic acid via gas phase oxidation of pinonic acid – a

mass spectrometric study of SOA aging, Atmos. Chem. Phys., 12, 1483-1496, 10.5194/acp-12-1483-2012, 2012.

Mentel, T. F., Kleist, E., Andres, S., Maso, M. D., Hohaus, T., Kiendler-Scharr, A., Rudich, Y., Springer, M., Tillmann, R., Uerlings, R., Wahner, A., and Wildt, J.: Secondary aerosol formation from stress-induced biogenic emissions and possible climate feedbacks, Atmos. Chem. Phys., 13, 8755-8770, 10.5194/acp-13-8755-2013, 2013.

Nguyen, T. B., Bates, K. H., Crounse, J. D., Schwantes, R. H., Zhang, X., Kjaergaard, H. G., Surratt, J. D., Lin, P., Laskin, A., Seinfeld, J. H., and Wennberg, P. O.: Mechanism of the hydroxyl radical oxidation of methacryloyl peroxynitrate (MPAN) and its pathway toward secondary organic aerosol formation in the atmosphere, Phys. Chem. Chem. Phys., 17, 17914-17926, 10.1039/C5CP02001H, 2015.

Offenberg, J. H., Lewis, C. W., Lewandowski, M., Jaoui, M., Kleindienst, T. E., and Edney, E. O.: Contributions of toluene and α-pinene to SOA formed in an irradiated toluene/α-pinene/NO_x/air mixture: Comparison of results using ^{14}C content and SOA organic tracer methods, Environ. Sci. Technol., 41, 3972-3976, 10.1021/es070089+, 2007.

Offenberg, J. H., Lewandowski, M., Edney, E. O., Kleindienst, T. E., and Jaoui, M.: Influence of aerosol acidity on the formation of secondary organic aerosol from biogenic precursor hydrocarbons, Environ. Sci. Technol., 43, 7742–7747, 10.1021/es901538e, 2009.

Ou, J., Yuan, Z., Zheng, J., Huang, Z., Shao, M., Li, Z., Huang, X., Guo, H., and Louie, P. K. K.: Ambient ozone control in a photochemically active region: Short-term despiking or long-term attainment?, Environ. Sci. Technol., 50, 5720–5728, 10.1021/acs.est.6b00345, 2016.

Paulot, F., Crounse, J. D., Kjaergaard, H. G., Kürten, A., St. Clair, J. M., Seinfeld, J. H., and Wennberg, P. O.: Unexpected epoxide formation in the gas-phase photooxidation of isoprene, Science, 325, 730-733, 10.1126/science.1172910, 2009.

Pye, H. O. T., Pinder, R. W., Piletic, I. R., Xie, Y., Capps, S. L., Lin, Y.-H., Surratt, J. D., Zhang, Z., Gold, A., Luecken, D. J., Hutzell, W. T., Jaoui, M., Offenberg, J. H., Kleindienst, T. E., Lewandowski, M., and Edney, E. O.: Epoxide pathways improve model predictions of isoprene markers and reveal key role of acidity in aerosol formation, Environ. Sci. Technol., 47, 11056-11064, 10.1021/es402106h, 2013.

Riva, M., Budisulistiorini, S. H., Zhang, Z., Gold, A., and Surratt, J. D.: Chemical characterization of

secondary organic aerosol constituents from isoprene ozonolysis in the presence of acidic aerosol, Atmos. Environ., 130, 5-13, 10.1016/j.atmosenv.2015.06.027, 2016.

Riva, M., Budisulistiorini, S. H., Zhang, Z., Gold, A., Thornton, J. A., Turpin, B. J., and Surratt, J. D.: Multiphase reactivity of gaseous hydroperoxide oligomers produced from isoprene ozonolysis in the presence of acidified aerosols, Atmos. Environ., 152, 314-322, 10.1016/j.atmosenv.2016.12.040, 2017.

Shen, R. Q., Ding, X., He, Q. F., Cong, Z. Y., Yu, Q. Q., and Wang, X. M.: Seasonal variation of secondary organic aerosol tracers in Central Tibetan Plateau, Atmos. Chem. Phys., 15, 8781-8793, 10.5194/acp-15-8781-2015, 2015.

Sipilä, M., Jokinen, T., Berndt, T., Richters, S., Makkonen, R., Donahue, N. M., Mauldin Iii, R. L., Kurtén, T., Paasonen, P., Sarnela, N., Ehn, M., Junninen, H., Rissanen, M. P., Thornton, J., Stratmann, F., Herrmann, H., Worsnop, D. R., Kulmala, M., Kerminen, V. M., and Petäjä, T.: Reactivity of stabilized Criegee intermediates (sCIs) from isoprene and monoterpene ozonolysis toward SO_2 and organic acids, Atmos. Chem. Phys., 14, 12143-12153, 10.5194/acp-14-12143-2014, 2014.

St. Clair, J. M., Rivera-Rios, J. C., Crounse, J. D., Knap, H. C., Bates, K. H., Teng, A. P., Jørgensen, S., Kjaergaard, H. G., Keutsch, F. N., and Wennberg, P. O.: Kinetics and products of the reaction of the first-generation isoprene hydroxy hydroperoxide (ISOPOOH) with OH, J. Phys. Chem. A., 120, 1441-1451, 10.1021/acs.jpca.5b06532, 2016.

Stone, E. A., Nguyen, T. T., Pradhan, B. B., and Man Dangol, P.: Assessment of biogenic secondary organic aerosol in the Himalayas, Environ. Chem., 9, 263-272, 10.1071/EN12002, 2012.

Surratt, J. D., Chan, A. W. H., Eddingsaas, N. C., Chan, M., Loza, C. L., Kwan, A. J., Hersey, S. P., Flagan, R. C., Wennberg, P. O., and Seinfeld, J. H.: Reactive intermediates revealed in secondary organic aerosol formation from isoprene, P. Natl. Acad. Sci. USA., 107, 6640-6645, 10.1073/P.Natl.Acad.Sci.USA.0911114107, 2010.

Szmigielski, R., Surratt, J. D., Gómez-González, Y., Van der Veken, P., Kourtchev, I., Vermeylen, R., Blockhuys, F., Jaoui, M., Kleindienst, T. E., Lewandowski, M., Offenberg, J. H., Edney, E. O., Seinfeld, J. H., Maenhaut, W., and Claeys, M.: 3-methyl-1,2,3-butanetricarboxylic acid: An atmospheric tracer for terpene secondary organic aerosol, Geophys. Res. Let., 34, 10.1029/2007gl031338, 2007.

Von Schneidemesser, E., Monks, P. S., Allan, J. D., Bruhwiler, L., Forster, P., Fowler, D., Lauer, A., Morgan, W. T., Paasonen, P., Righi, M., Sindelarova, K., and Sutton, M. A.: Chemistry and the linkages between air quality and climate change, Chem. Rev., 115, 3856-3897, 10.1021/acs.chemrev.5b00089,

2015.

Wang, W., Kourtchev, I., Graham, B., Cafmeyer, J., Maenhaut, i., and Claeys, M.: Characterization of oxygenated derivatives of isoprene related to 2-methyltetrols in Amazonian aerosols using trimethylsilylation and gas chromatography/ion trap mass spectrometry, Rapid Commun. Mass Spectrom., 19, 1343-1351, 10.1002/rcm.1940, 2005.

Wang, X., Liu, H., Pang, J., Carmichael, G., He, K., Fan, Q., Zhong, L., Wu, Z., and Zhang, J.: Reductions in sulfur pollution in the Pearl River Delta region, China: Assessing the effectiveness of emission controls, Atmos. Environ., 76, 113-124, 10.1016/j.atmosenv.2013.04.074, 2013.

Watanabe, A. C., Stropoli, S. J., and Elrod, M. J.: Assessing the potential mechanisms of isomerization reactions of isoprene epoxydiols on secondary organic aerosol, Environ. Sci. Technol., 52, 8346-8354, 10.1021/acs.est.8b01780, 2018.

Worton, D. R., Surratt, J. D., LaFranchi, B. W., Chan, A. W. H., Zhao, Y., Weber, R. J., Park, J.-H., Gilman, J. B., de Gouw, J., Park, C., Schade, G., Beaver, M., Clair, J. M. S., Crounse, J., Wennberg, P., Wolfe, G. M., Harrold, S., Thornton, J. A., Farmer, D. K., Docherty, K. S., Cubison, M. J., Jimenez, J.-L., Frossard, A. A., Russell, L. M., Kristensen, K., Glasius, M., Mao, J., Ren, X., Brune, W., Browne, E. C., Pusede, S. E., Cohen, R. C., Seinfeld, J. H., and Goldstein, A. H.: Observational insights into aerosol formation from isoprene, Environ. Sci. Technol., 47, 11396–11402, 10.1021/es4011064, 2013.

Xu, L., Guo, H., Boyd, C. M., Klein, M., Bougiatioti, A., Cerully, K. M., Hite, J. R., Isaacman-VanWertz, G., Kreisberg, N. M., Knote, C., Olson, K., Koss, A., Goldstein, A. H., Hering, S. V., de Gouw, J., Baumann, K., Lee, S.-H., Nenes, A., Weber, R. J., and Ng, N. L.: Effects of anthropogenic emissions on aerosol formation from isoprene and monoterpenes in the southeastern United States, P. Natl. Acad. Sci. USA., 112, 37-42, 10.1073/ P.Natl.Acad.Sci.USA.1417609112, 2015.

Xu, L., Middlebrook, A. M., Liao, J., de Gouw, J. A., Guo, H., Weber, R. J., Nenes, A., Lopez-Hilfiker, F. D., Lee, B. H., Thornton, J. A., Brock, C. A., Neuman, J. A., Nowak, J. B., Pollack, I. B., Welti, A., Graus, M., Warneke, C., and Ng, N. L.: Enhanced formation of isoprene-derived organic aerosol in sulfur-rich power plant plumes during Southeast Nexus, J. Geophys. Res-Atmos., 121, 11137-11153, 10.1002/2016JD025156, 2016.

Ye, J., Abbatt, J. P. D., and Chan, A. W. H.: Novel pathway of SO_2 oxidation in the atmosphere: Reactions with monoterpene ozonolysis intermediates and secondary organic aerosol, Atmos. Chem. Phys., 18, 5549-5565, 10.5194/acp-18-5549-2018, 2018.

572 Zhang, R. Y., Wang, G. H., Guo, S., Zarnora, M. L., Ying, Q., Lin, Y., Wang, W. G., Hu, M., and Wang,
573 Y.: Formation of urban fine particulate matter, Chem. Rev., 115, 3803-3855,
574 10.1021/acs.chemrev.5b00067, 2015.
575 Zheng, J., Zheng, Z., Yu, Y., and Zhong, L.: Temporal, spatial characteristics and uncertainty of biogenic
576 VOC emissions in the Pearl River Delta region, China, Atmos. Environ., 44, 1960-1969,
577 10.1016/j.atmosenv.2010.03.001, 2010.
578

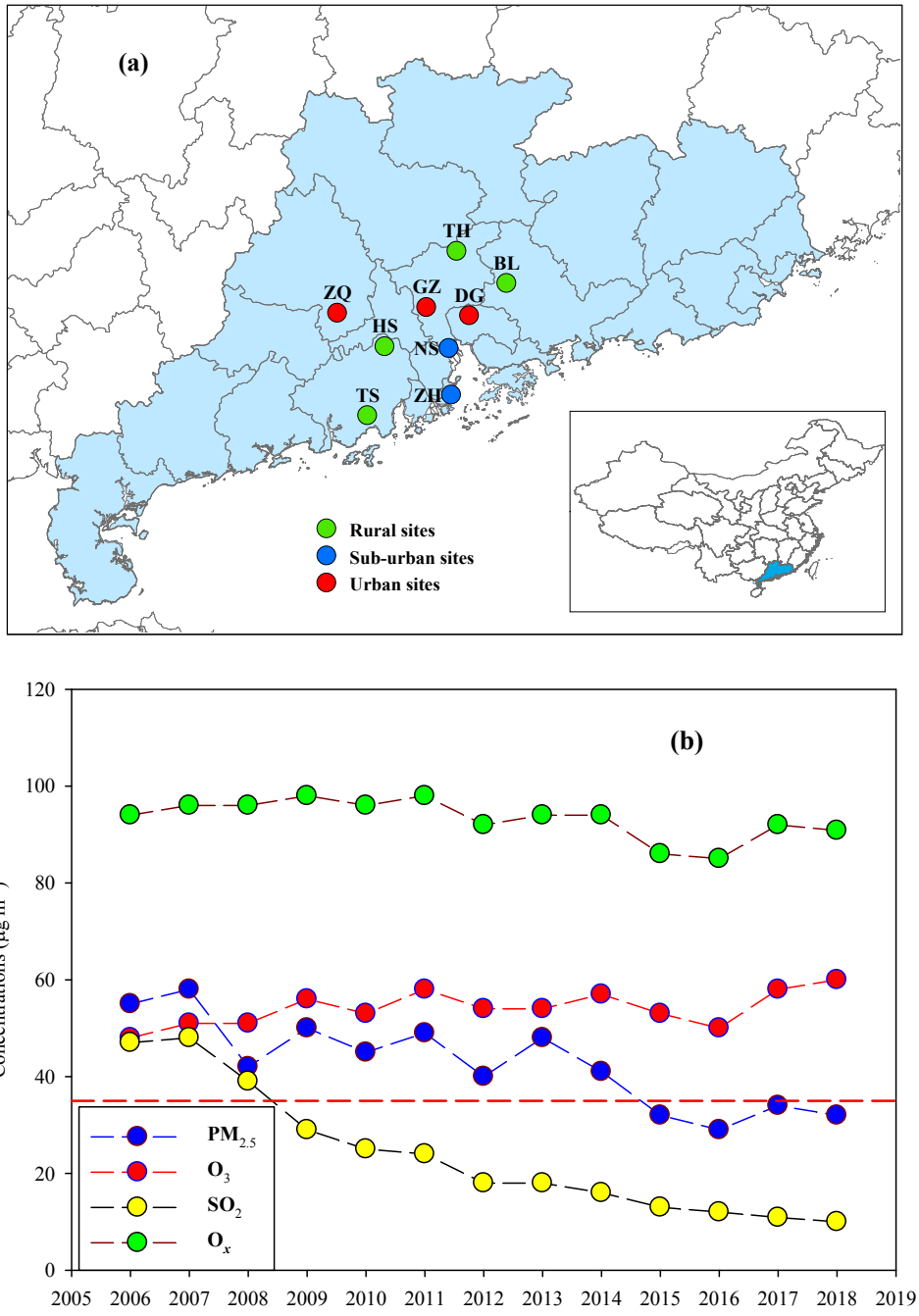

579

580

581 Figure 1 Sampling sites in the PRD (a) and long-term trends of annual-mean $PM_{2.5}$, O_3, SO_2 and O_x recorded by the

582 Guangdong-Hong Kong-Macao regional air quality monitoring network (http://www.gdep.gov.cn/hjjce/) (b). The

583 red dash line indicates the NAAQS for annual-mean $PM_{2.5}$ concentrations (35 μg m^{-3}).

584

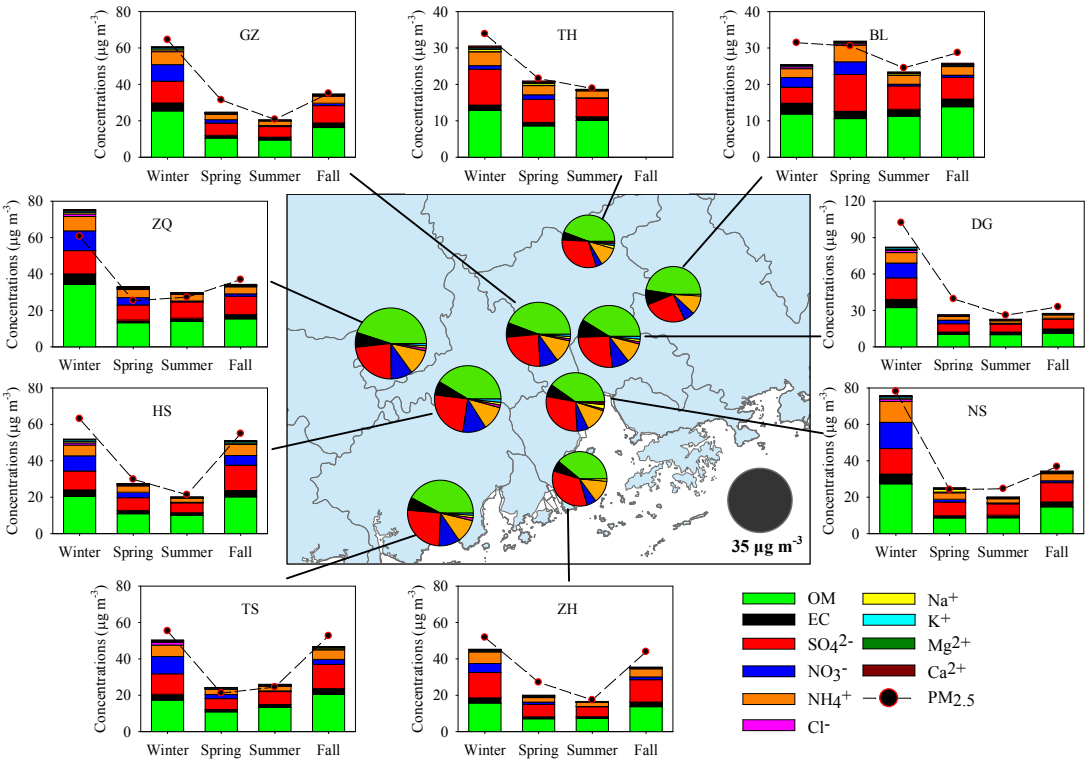

585

586 Figure 2 Major components in $PM_{2.5}$ and their seasonal variation at 9 sites. The pie charts in the central figure
587 represent the annual average of major components. High levels of $PM_{2.5}$ and major components were observed in
588 wintertime.

589

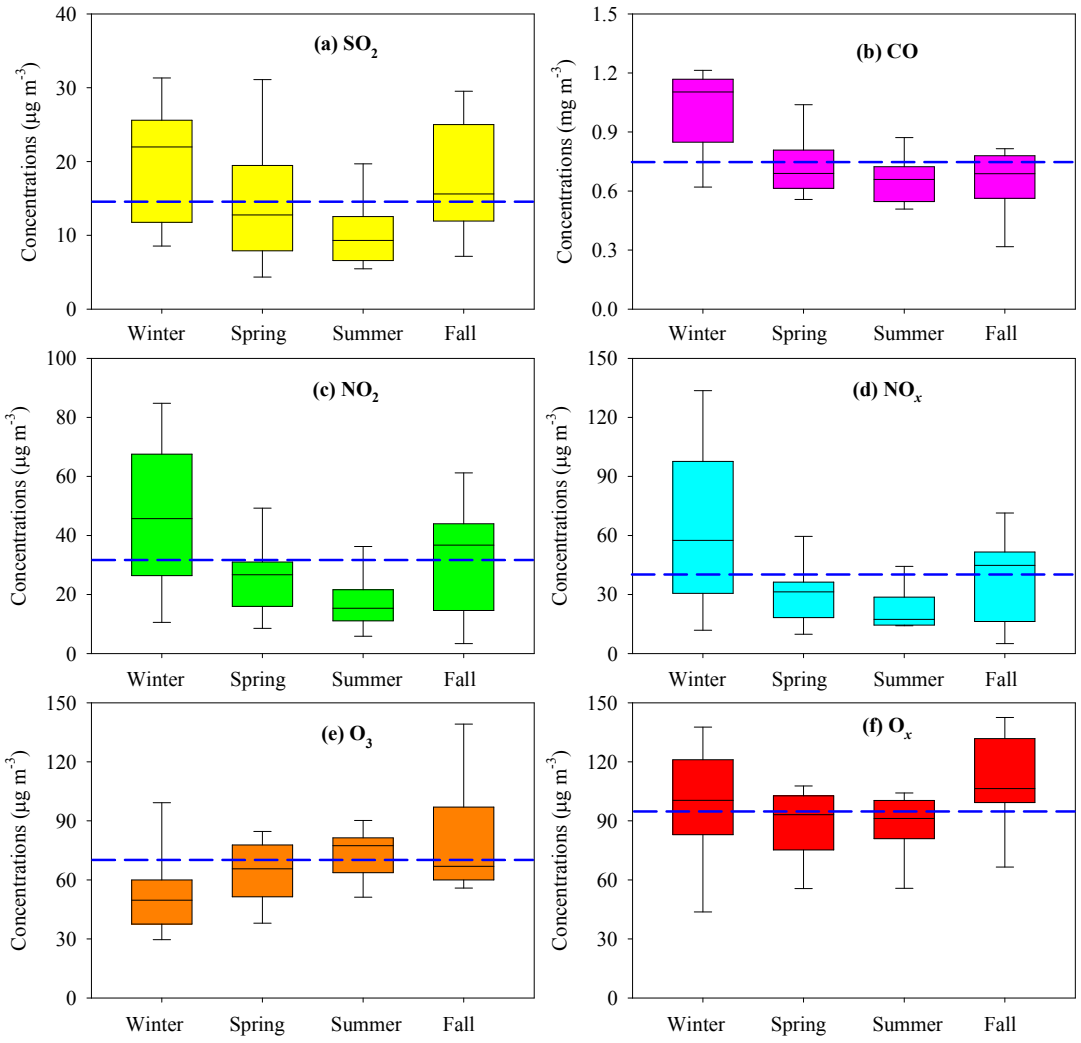

590

591 Figure 3 Seasonal variation of gaseous pollutants in the PRD. Box with error bars represent 10^{th}, 25^{th}, 75^{th}, 90^{th}
592 percentiles for each pollutant. The line in each box represents the median value. Blue dash lines indicate annual
593 average concentrations of SO_2 (14.9 μg m^{-3}), CO (0.74 mg m^{-3}), NO_2 (28.5 μg m^{-3}), NO_x (39.0μg m^{-3}), O_3 (67.7 μg
594 m^{-3}) and O_x (96.1 μg m^{-3}).

595

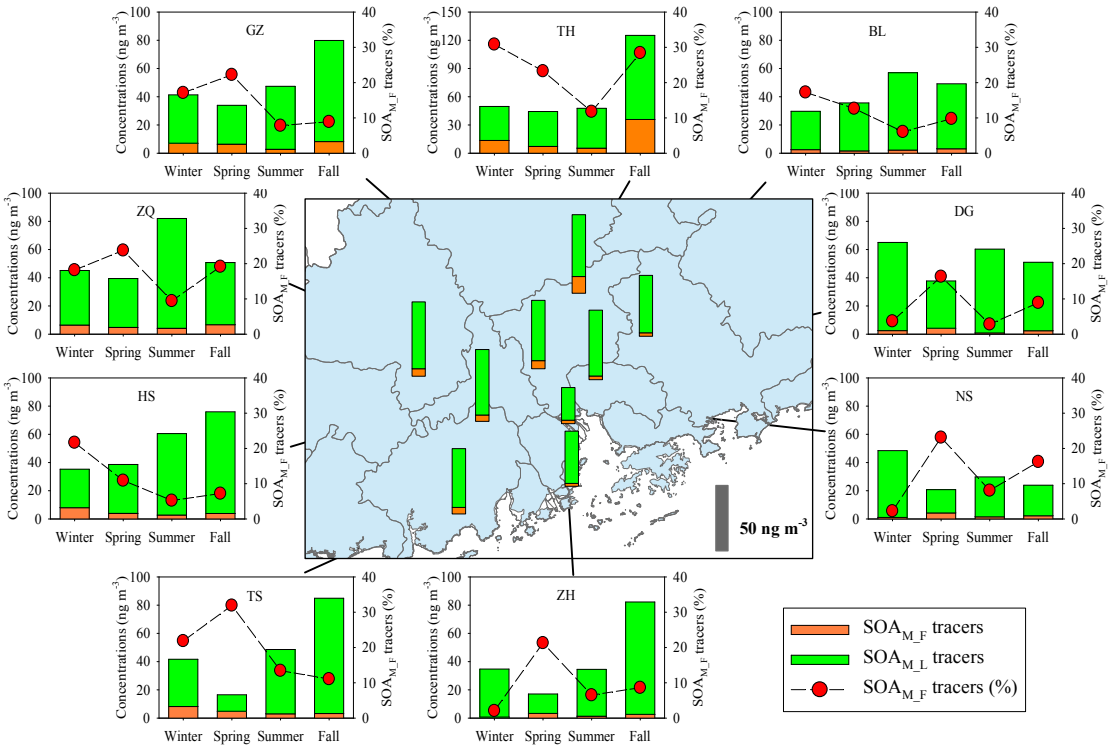

596

597 Figure 4 Spatial and seasonal variations of SOA_M tracers at 9 sites in the PRD. The bars in the central figure represent

598 the annual average concentrations of the SOA_M tracers.

599

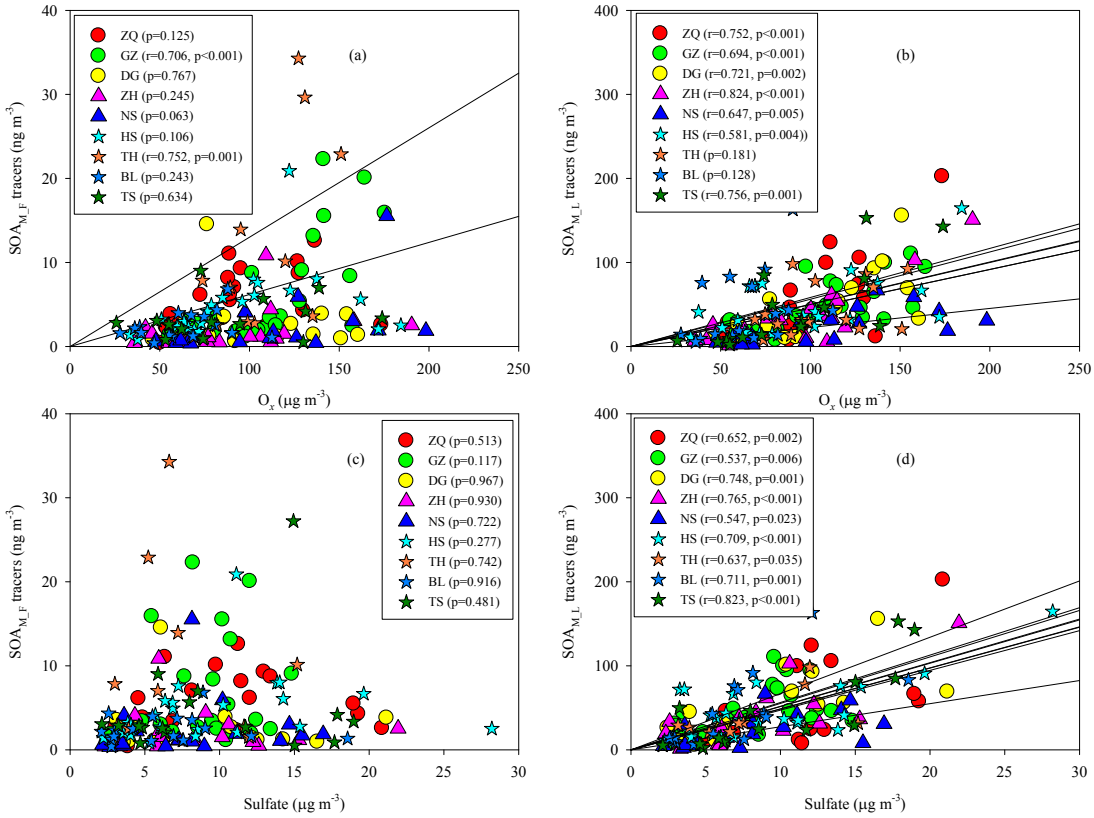

600

601 Figure 5 Correlations of SOA_{M_F} and SOA_{M_L} tracers with O_x (a, b) and sulfate (c, d)

602

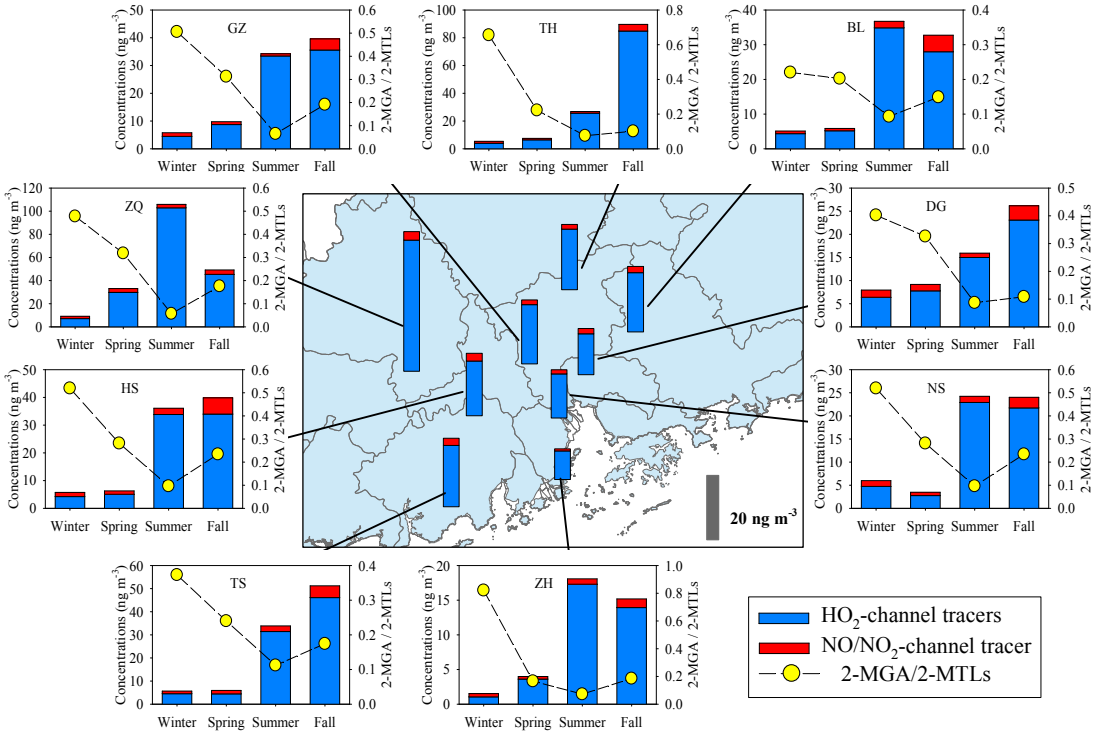

603

604 Figure 6 Spatial and seasonal variations of SOA_I tracers at 9 sites in the PRD. The bars in the central figure represent

605 the annual average concentrations of the SOA_I tracers.

606

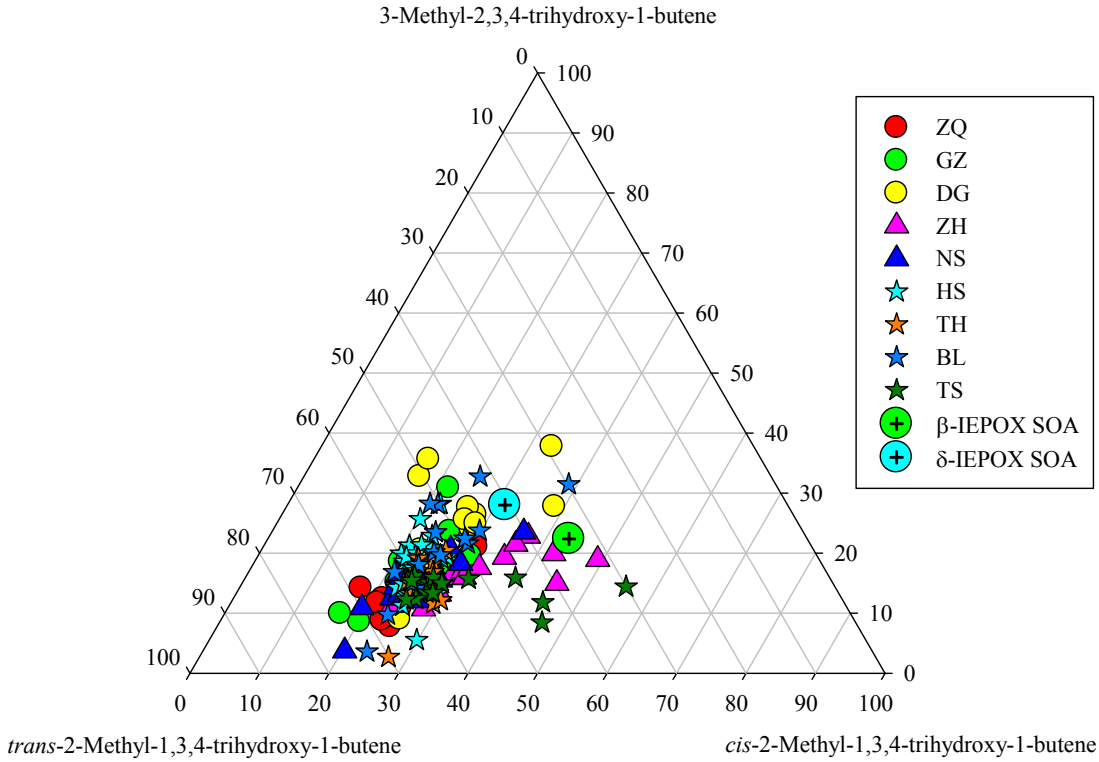

607

608 Figure 7 Ternary plot of C_5-alkene triol isomers in the PRD samples and in the β-IEPOX and δ-IEPOX derived
609 SOA (Lin et al., 2012).

610

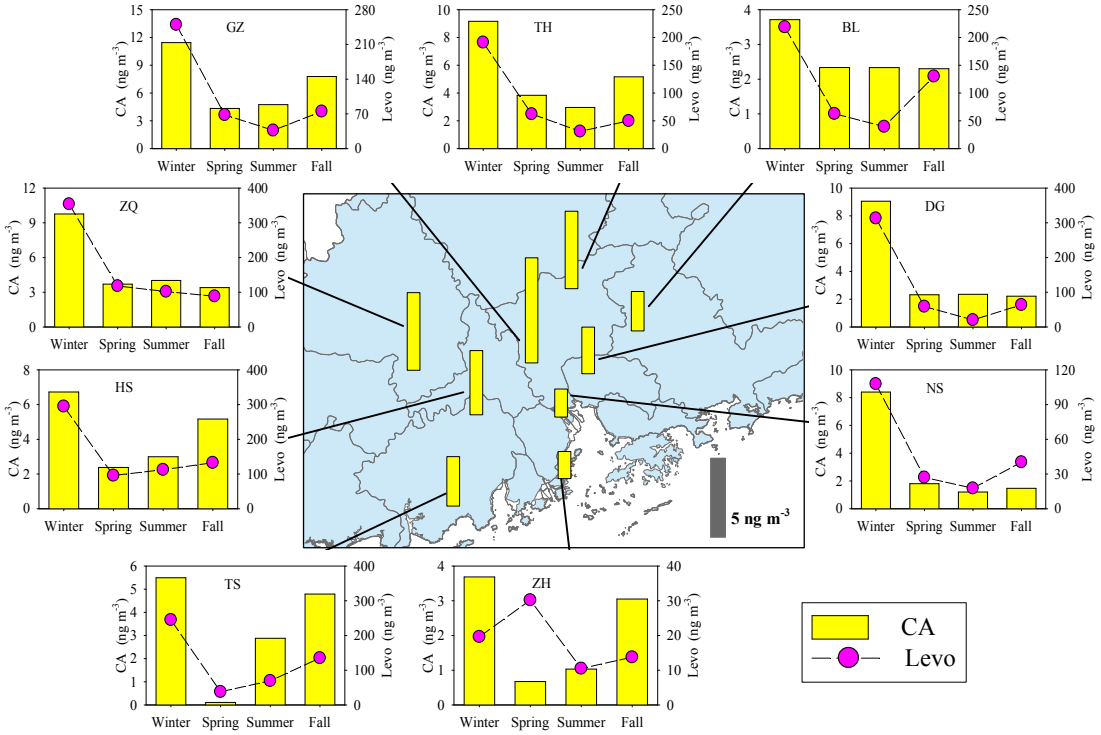

611

612 Figure 8 Spatial and seasonal variations of SOA_c tracer (CA) at 9 sites in the PRD. The bars in the central figure
613 represent the annual average concentration of the SOA_c tracers. The pink circle indicates the BB tracer, levoglucosan
614 (Levo).

615

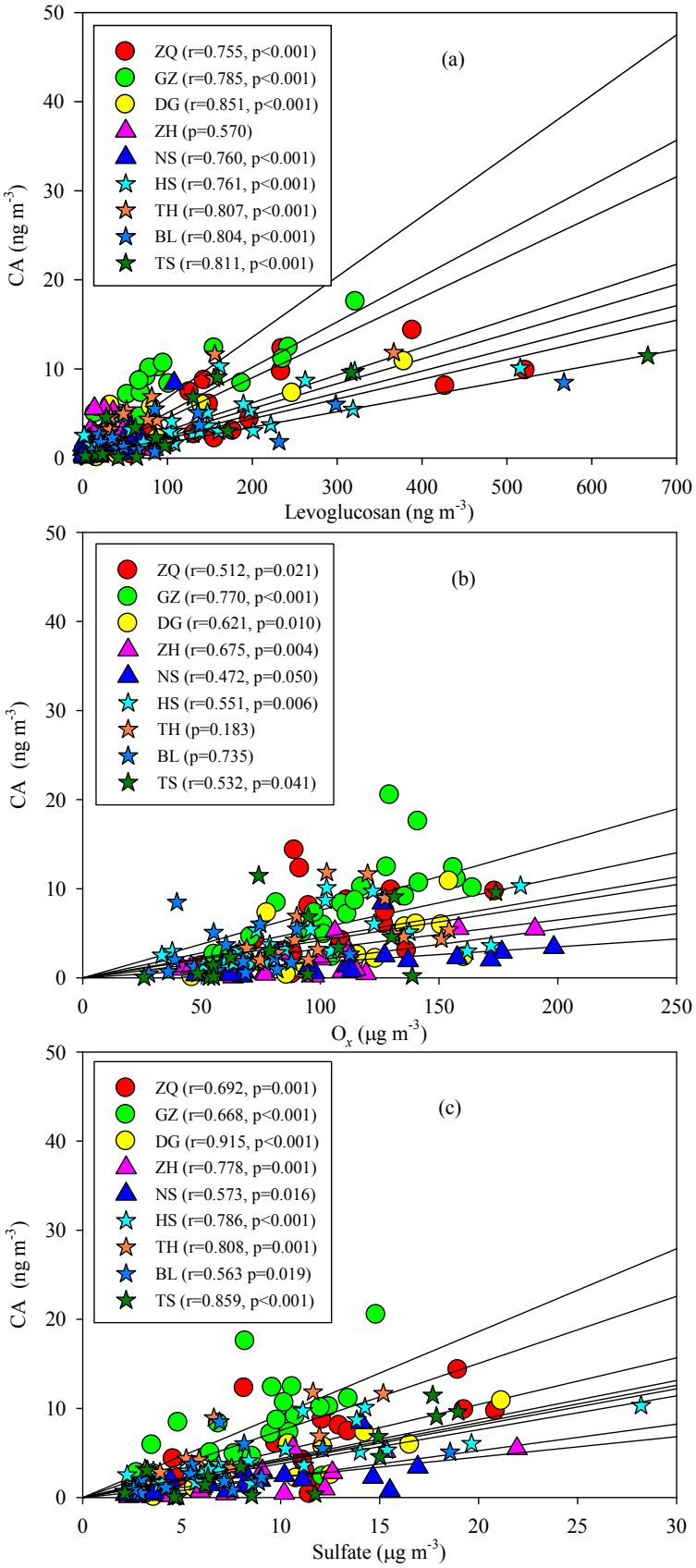

Figure 9 Significant correlations of CA with levoglucosan (a), O_x (b) and sulfate (c).

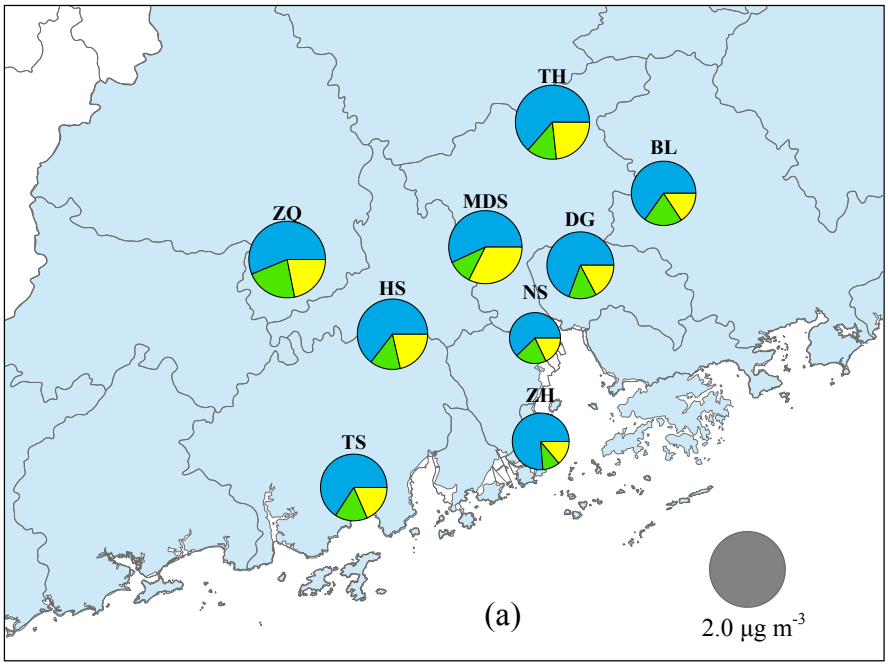

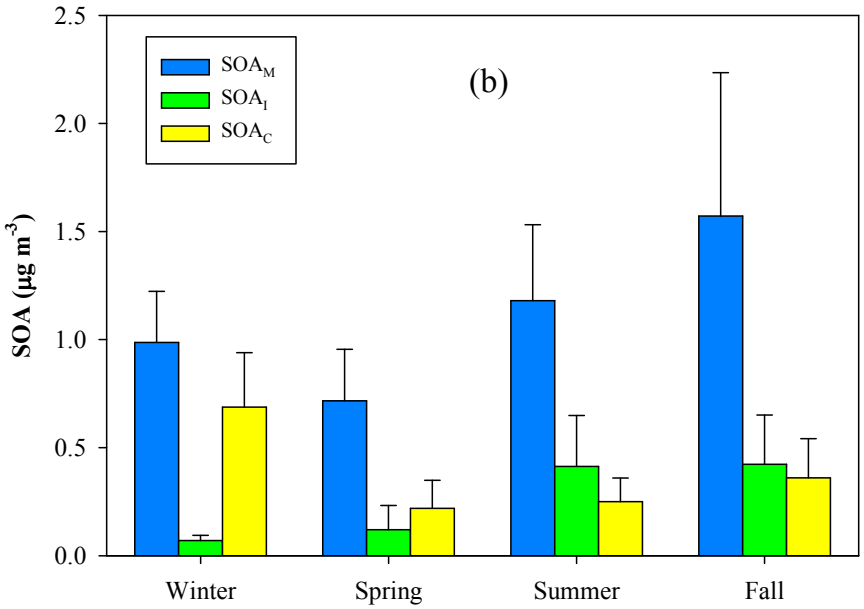

Figure 10 Spatial (a) and seasonal (b) variations in BSOA components

624 Table 1 Correlations between SOA_I tracers and NO_x

	2-MGA		2-MGA/2-MTLs	
	Coefficient (r)	*p*-value	Coefficient (r)	*p*-value
NO	0.028	0.733	0.166	0.043
NO_2	0.205	0.008	0.352	<0.001
NO_x	0.132	0.102	0.286	<0.001
NO_2/NO	0.001	0.986	0.162	0.048

625

626 Table 2 Correlations of BSOA with sulfate and O_x

	Sulfate			O_x		
	Slope	*p*-value	% [a]	Slope	*p*-value	% [a]
SOA_M	0.112	<0.001	45	0.013	<0.001	57
SOA_I	0.020	<0.001	34	0.003	<0.001	50
SOA_C	0.041	<0.001	46	0.004	<0.001	55
BSOA	0.172	<0.001	44	0.019	<0.001	55

627 [a] Percentages of SOA reduction at 50% decline of sulfate or O_x

628